2022

Development and Experimental Validation of a Mechanistic Chamber Model of a Novel Peristaltic Compressor

MAZHARUL ISLAM

Jeffery Nicholas

Craig R Bradshaw

Development and Experimental Validation of a Mechanistic Chamber Model of a Novel Peristaltic Compressor

Mazharul ISLAM[(1)], Jeffery NICHOLAS[(2)], Craig R. BRADSHAW[(3)]

Oklahoma State University, Mechanical & Aerospace Engineering,
Stillwater, OK 74078, USA

[(1)]mazharul.islam10@okstate.edu, [(2)]jeffery.nicholas@okstate.edu [(3)]craig.bradshaw@okstate.edu.

ABSTRACT

This work presents the novel peristaltic compressor, which has the potential to improve compressor efficiency by eliminating losses due to valves and over/under compression. This work builds on previous work by presenting a modified mechanistic chamber model of a prototype compressor along with operational updates to the reconfigurable prototype, and validation of the model through experimental data with air as the working fluid. A mathematical model is presented to add diaphragm flexibility to the geometry of the compression chamber that is coupled with the mass and energy conservation equations in the mechanistic chamber model. The reconfigurable prototype is operated with volume ratios ranging from 1.5 to 9 at pressure ratios ranging from 1 to 2.5. Each test is repeated 6 times and experimental uncertainty of each test is within 4%. The mechanistic chamber model of a peristaltic compressor predicts the experimental mass flow rate and volumetric efficiency within 10% MAPE.

1. INTRODUCTION

The United States ranks second in the world for energy consumption, using nearly 100 quadrillion BTUs (quad) in 2019 (U.S. EIA, 2019) and a significant amount of this energy is consumed by compression. Roughly 24% of the 100 quad is allocated towards refrigeration and air-conditioning units utilizing a standard vapor-compression cycle (U.S. EIA, 2018). The energy consumption of a vapor compression cycle is highly dependent on the compressor, which accounts for nearly 80% of the energy in most systems. (Ahamed *et al*., 2011). Additionally, in industry, 10-30% energy is consumed during the generation of compressed air and it is one of the major sources of excessive energy use (U.S. DOE, 2004). Based on these applications, any improvements to compressor efficiency can potentially have a large impact on total energy use.

Traditional positive displacement compressors require valves, internal volume ratios, or both to operate. These two features generate the majority of the losses in compressors (Pearson, 2015). Developing a compressor that can reduce or remove these losses and that can be integrated into the industry to provide a significant advantage over previous technologies. The peristaltic compressor mechanism utilizes mechanical actuation that moves an elastic diaphragm in a motion such that compresses a fluid by using a series of segmented pockets. These pockets motivate fluid flow and allow a user to adjust the volume ratio on-the-fly. Furthermore, this removes the necessity of a valve, eliminating porting losses. This is functionally similar to a scroll compressor, using a series of segmented compression pockets, but a scroll compressor operates with a fixed volume ratio. Previous work has demonstrated the potential of the peristaltic compressor to operate without valves and at variable volume ratios, (Sulfridge & Miller, 2001, Lawless *et al.*, 1987). Additionally, it can also be integrated as a pump, to move fluids from one location to the desired location (Huang et al., 2006, Hartley, 1999).

None of the previous studies developed a thermodynamic model and compared the model with experimental analysis to explore the potential of the peristaltic mechanism for industrial applications. This paper continues the work from Islam & Bradshaw (2021) and modifies the preliminary thermodynamic model of the compressor and validate the model with the experimental results. The mechanistic chamber model is used to add additional physics to improve the geometric model for the compression chamber. The reconfigurable prototype is used to collect a significant amount of data to check the repeatability of the compressor and validate the mechanistic chamber model.

2. PERISTALTIC COMPRESSOR MODEL

The overall goal of this study is to determine the thermodynamic potential and volumetric performance of the novel peristaltic compressor. To accomplish this objective, a computational model and a prototype compressor have been created to study the influence of variable volume ratios, valveless operation, and easily reconfigure the geometry of the peristaltic compressor. A schematic of the proposed reconfigurable peristaltic compressor prototype is shown in Figure 1. To place the load on the diaphragm for actuating the flow in the compressor, a series of linear actuators are utilized in the design. A cylindrical compression chamber is created by constraining and sealing the diaphragm against a female die. The linear actuator is connected to a male die (piston) that presses the diaphragm against the female die, compressing the chamber while sealing it, simultaneously. The mass flow of the compression chamber is controlled by 10 linear actuators in the design where a piston (male die) is attached to each device. The pistons depress the diaphragm in a specified sequence to move and compress the fluid.

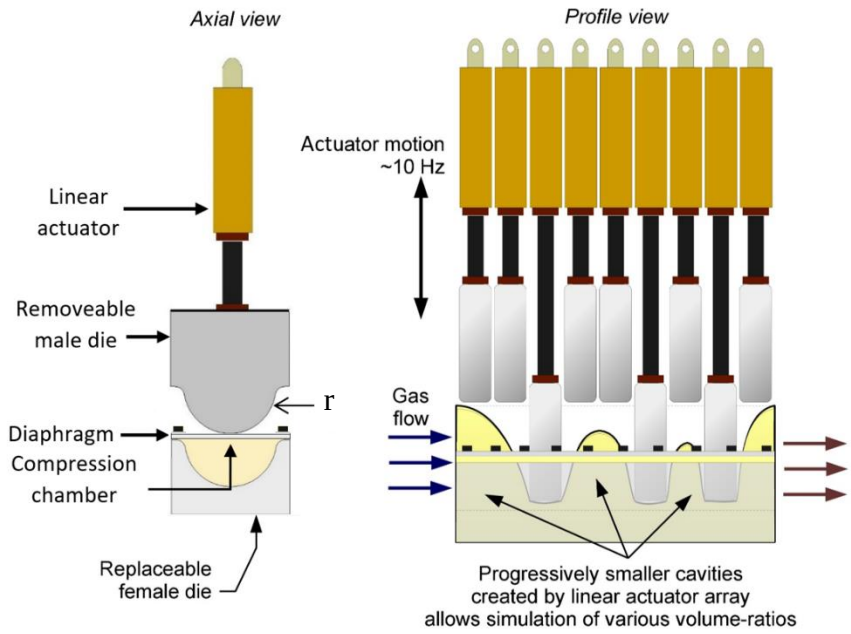

Figure 1: A scheme of the proposed reconfigurable peristaltic compressor prototype (Bradshaw, 2017).

A model for a novel compressor is needed to determine the thermodynamic properties of the working fluid in the compression chamber at any point during the compression process. The properties will assist to estimate the efficiency and capacity of the system. Additionally, the model will help to evaluate the working behavior of the system to develop a more effective compressor. To build the thermodynamic model of the peristaltic compressor, a mechanistic chamber model approach is considered which is similar to the models presented by Bell *et al*. (2020) and Tanveer & Bradshaw (2020). The mechanistic chamber model uses a series of sub-models to solve the geometry, mass and energy balance equations to evaluate the target parameters. The sub-models of the solver evaluate the properties of the compression chamber at every step. The final temperature and density of the cycle are used to converge the solver. Once the residuals are smaller than the tolerance, the model proceeds to the next step. Or else, the model will be repeated by acquiring the final temperature and density as the system's new initial values. After the compression process solver, the wall temperature of the compression chamber is considered to balance the heat transfer from the boundary to the ambient (Islam & Bradshaw, 2021).

2.1 Geometric Model

The instantaneous volume of the compression chamber is required for the mass and energy balance equations. From Islam *et al.* (2021), we observe that the semi-circular compression chamber creates a constant control volume. It means when the diaphragm remains flat on the female die as shown in Figure 2, the diaphragm rebounds properly during the linear actuation. In the previous work, we have considered the diaphragm is very flexible and the piston pressing the

diaphragm as two circles intersecting each other. In the reality, the diaphragm is behaving in a different manner which we have to consider to make the model more efficient and accurate. For that reason, it has been investigated how deflection occurs when a piston presses a flat elastic diaphragm to produce cylindrical bending. Timoshenko & Krieger (1941) introduced an approach to calculate the cylindrical deflection of an elastic rectangular membrane when a load is acting on the membrane and the membrane is fixed rigidly such that it cannot rotate. Figure 2 demonstrates how a single piston load deflects the diaphragm.

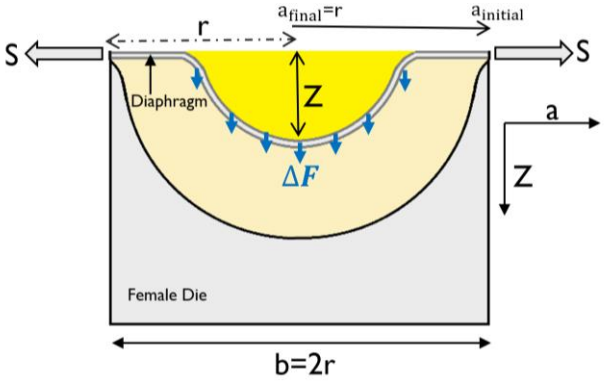

Figure 2: Cross-sectional schematic of a compression chamber when piston load deflects the diaphragm.

In the compressor, the piston is deflecting the diaphragm in the same manner. Therefore, to calculate the deflection of the elastic diaphragm, we derive an equation by using the approach. The area and volume of the defected segment can be defined by using the deflection length. The following equation is derived to calculate the displacement of the elastic diaphragm,

$$Z = \frac{\Delta F b^4}{16 D u_g{}^3 \tanh u_g}\left\{\frac{\cosh[u_g\left(1-\frac{2a}{b}\right)]}{\cosh u_g} - 1\right\} + \frac{\Delta F b^2 (b-a) a}{8 D u_g{}^2}, \tag{1}$$

where Z is the deflection length of the diaphragm when increasing load, ΔF is acting on it. The total length of the diaphragm is b=2r where r is the semi-circle's radius. Moreover, a change from $a_{final} = r$ to $a_{initial} \approx 0$. This means when there is no load and deflection (Z=0), $a = a_{final}$ and when $a = a_{initial}$, will have maximum deflection. For equation 1, flexural rigidity, D has to be determined by using,

$$D = \frac{E\, t^3}{12\,(1-\mu^3)}. \tag{2}$$

The flexural rigidity will need to calculate the function u_g, where,

$$u_g = \sqrt{\frac{S\, b^2}{4\, D}}. \tag{3}$$

From equation 1, we can calculate the area of the deflected segment by the following expression,

$$A_d = 2\int_{a_{initial}}^{a_{final}} Z\, da. \tag{4}$$

By increasing the deflection, Z the area of the deflected segment, A_d will increase. Thus, the area of the compression chamber is

$$A_C = \frac{1}{2}\pi r^2 - A_d, \tag{5}$$

and the volume of the compression chamber during the piston load is

$$V = A_C Y. \tag{6}$$

The equations can define the behavior of the control volume for a single-piston load. In the design, we are considering 10 pistons to operate the diaphragm and compress the working fluid. By using the geometric terms, the model calculates the total volume of the compression chamber, where pistons 1 through 9 press the diaphragm, sequentially. At the end, all pistons return to their home state to pull the working fluid, allowing the fluid to reach its initial volume. Figure 3 shows how the volume of the compression chamber changes when a single piston acts on the diaphragm (Fig 3a) and all the pistons act during one compression cycle (Fig 3b).

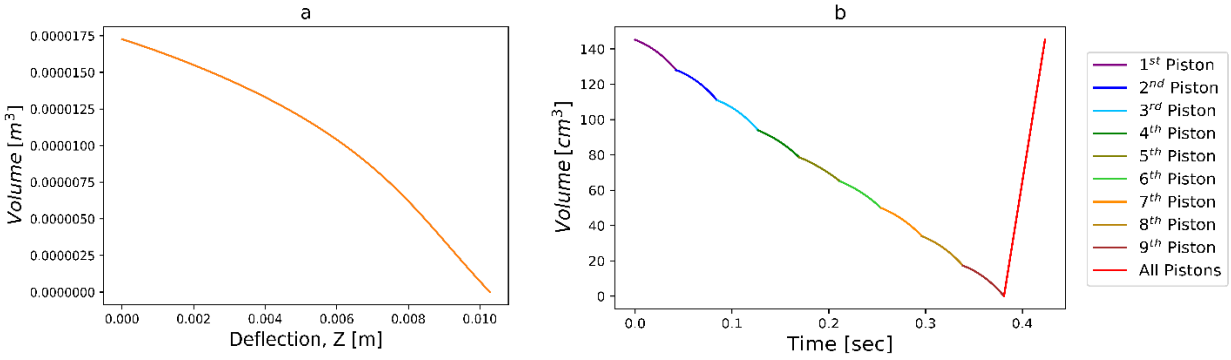

Figure 3: a) Volume change as a function of deflection when single-piston acts on the diaphragm, b) Volume of the compression chamber as a function of time

The sequential operation can create a discrete number of different volume ratios in various modes of sequencing as shown in (Islam & Bradshaw, 2021). This work will focus on the first mode from (Islam & Bradshaw, 2021), which for the existing prototype with 10 pistons can produce volume ratios from 1.5 to 9. The term Pivotal Piston (PP) is introduced to define different volume ratios, by indicating the piston that compression is complete.

2.2 Compression Processes Equations, Mass-flow and Leakage Model

The geometry model is coupled with the compression process equations presented in Islam & Bradshaw, 2021 and extracts the instantaneous volume of the compression chamber. Heun's method is used to determine the temperature and density. By using these two independent variables other thermodynamic properties, such as pressure and enthalpy, can be determined with Coolprop (Bell *et al.*, 2014). The mass and energy balance equations also require specific information as input, such as the mass flow rate.

Mass flow models will determine how fluid moves through the inlet and outlet of the compressor. Mass flow rates of the model at discharge, $\dot{m}_{out}$, are dependent on the discharge pressure and pivotal piston position. The term "$\dot{m}_{out}$" occurs when the pressure and volume of the compression chamber meet the discharge pressure and discharge volume condition at the same time. On the other hand, when all of the pistons start moving upward to fill the chamber with fluid and pressure of the compression chamber would be greater than suction pressure, the mass flow rate of the model at suction, $\dot{m}_{in}$ occurs. The following expression is used to calculate the mass flow rate:

$$\dot{m} = \rho A_s \sqrt{(\gamma R_g T)\left(\left(\frac{P_{low}}{P_{high}}\right)^{\left(-\frac{\gamma-1}{\gamma}\right)} - 1\right)\left(\frac{2}{\gamma-1}\right)}. \quad (7)$$

The leakage model only focuses on the leakage gap between the diaphragm and the female die at the inlet and outlet when the piston is fully engaged. For the leakage gap, a specific height (25 µm) at the inlet and the outlet is considered. The gap size determines the leakage mass flow rate which influences the net mass flow rate. The following equation is used to determine the leakage mass flow rate at the inlet, $\dot{m}_{leak1}$ and outlet, $\dot{m}_{leak2}$,

$$\dot{m}_{leak1} = \dot{m}_{leak2} = \rho \vartheta A_l. \quad (8)$$

The leakage gaps at the inlet and outlet ports have a positive impact on the model results. Figure 6 illustrates leakage occurring in the model. Suction and discharge pressure and the discharge volume (V_{dis}) would decide when the inlet ($\dot{m}_{in}$), outlet ($\dot{m}_{in}$) and leak ($\dot{m}_{leak1}, \dot{m}_{leak2}$) mass flow rates happen in the system. Figure 4 illustrates the

computational algorithm for the mass flow rate where P and V are pressure and volume of the compression chamber, respectively.

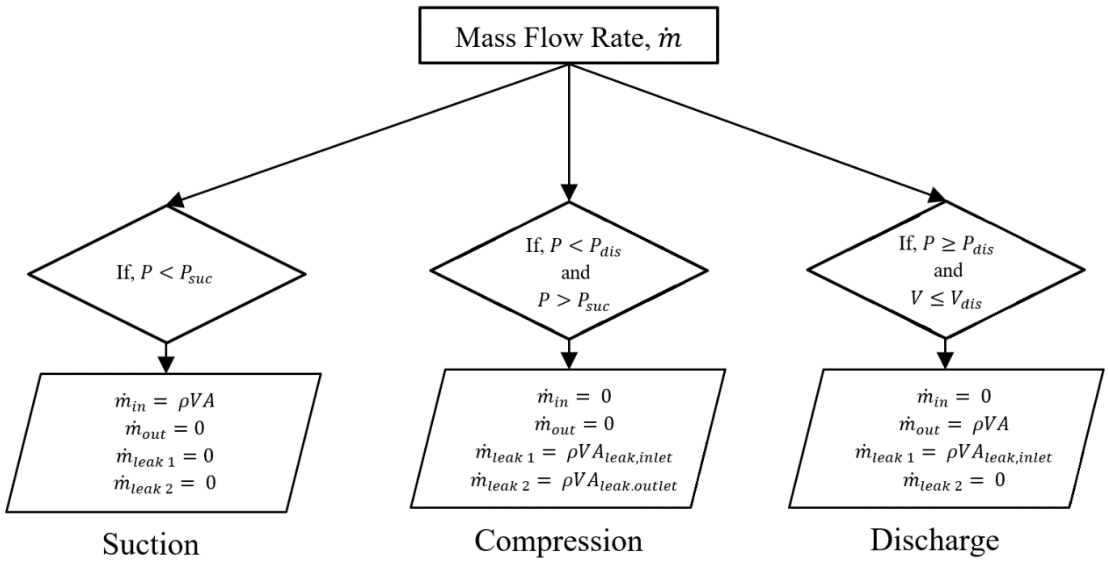

Figure 4: Computational algorithm for the mass flow rate.

3. RECONFIGURABLE PROTOTYPE AND PERFORMANCE ANALYSIS

The novel peristaltic compressor utilizes a set of 10 linearly actuating pistons that compresses the working fluid creating an operator-desired pressure ratio. This prototype has been set up to accommodate differing lab set-ups for mobility and ease of testing. In the compression section, a neoprene rubber diaphragm is mounted under the actuators to allow for the peristaltic compression of the working fluid. For the experiment air is used as working fluid. A mass flow meter, two pressure transducers, and two resistance temperature detectors (RTD) are used to measure the inlet and outlet conditions (Islam *et al.*, 2021). Figure 5 presents the physical reconfigurable prototype peristaltic compressor.

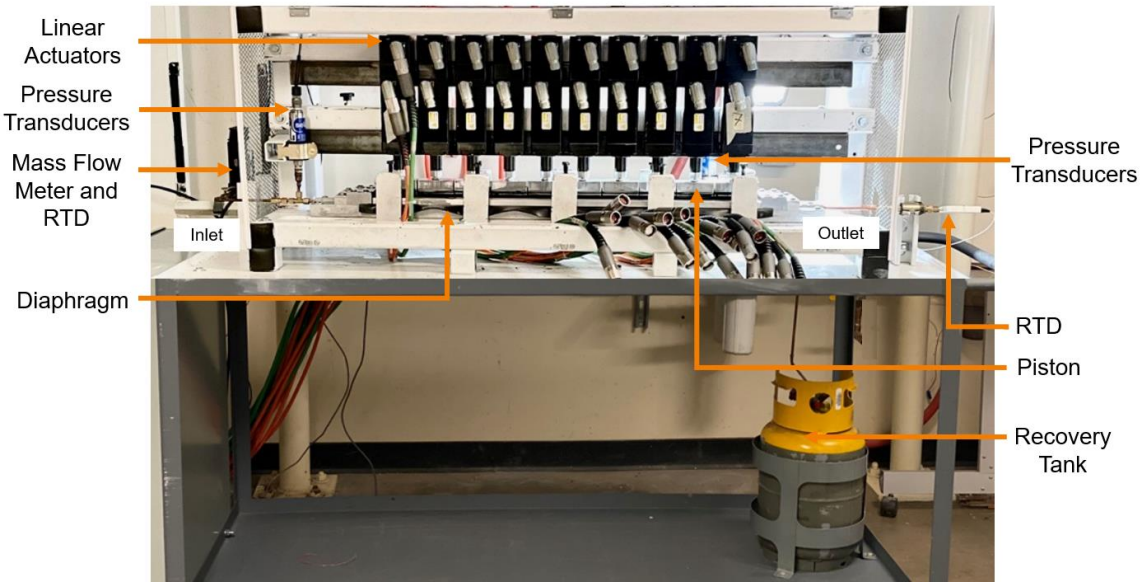

Figure 5: Experimental Set up.

3.1 Test Matrix

The test matrix includes six different pivotal piston conditions ranging from pivotal positions four to nine, representing volume ratios that range from 1.5 to 9. For each pivotal piston, the compressor is operated at various pressure ratios, controlled by the position of an outlet metering valve. There are four metering valve conditions tested to adjust the pressure ratio, resulting in quantities varying from 1.02 to 2.2. For each metering valve position, six tests are conducted and averaged. The standard deviation, 95% confidence interval, and mass flow uncertainty of the six runs are calculated. Additionally, the mass flow rate, density, inlet and outlet pressure, and temperature are collected and recorded in this matrix. Each diaphragm is serialized and the stage of life (*i.e.* cumulative operational time) in which the diaphragm is operating is noted. In summary, for each of the 9 pivotal pistons, 24 tests are conducted resulting in a total of 144 raw data points collected and netting 24 averaged data points.

3.2 Repeatability and Experimental Uncertainty

To calculate the experimental uncertainty for each test matrix, a student's t-distribution calculation is conducted. This calculation is used to find the 95% confidence interval across each of the 24 averaged data points. Using this method, a maximum and minimum bound for the 95% confidence interval is found and the range between these two quantities is calculated. This range is then added in the quadrature with the systematic uncertainty of the mass flow meter which then generates the total uncertainty. From the experimental results, the mean mass flow uncertainty is 0.042 grams/second. According to manufacturer data, the mass flow meter uncertainty allows for 0.040 grams/second. Figure 6, presents the final data collected, including the mass flow rate and temperature ratio as a function of pressure ratio. It can be observed that the results follow similar trends, even at differential pivotal pistons.

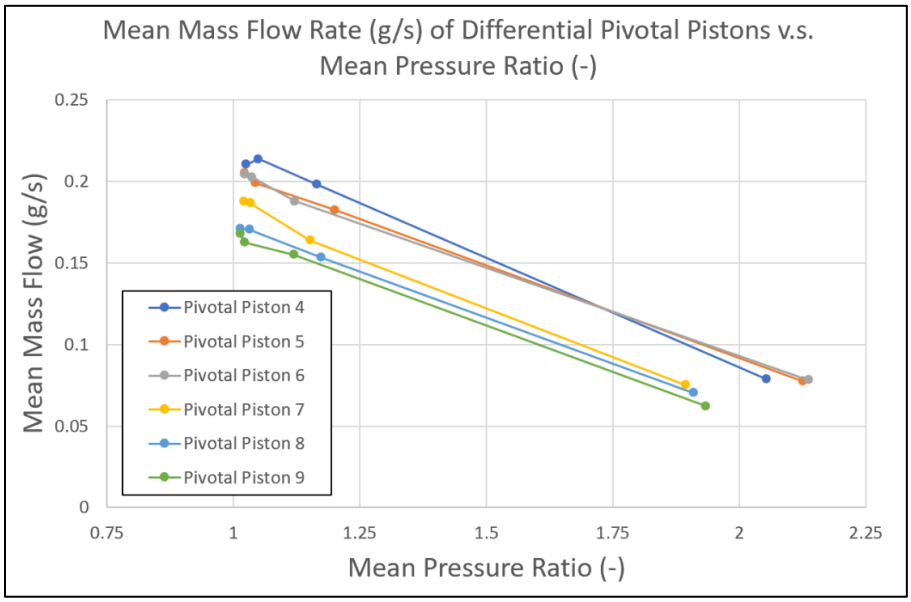

Figure 6: Overall repeatability data with mean mass flow plotted as a function of pressure ratio.

4. PERISTALTIC COMPRESSOR MODEL VALIDATION

The experimental results are compared with the computational compressor model. The experimental testing imposed an inlet air state, volume and pressure ratio on the compressor and measured the resulting mass flow rate. The model predicted mass flow rate is compared against the experimental results and error quantified. It is typical in mechanistic chamber models to require tuning of the mass flow rate using a tuning coefficient (C_{leak}) of the form,

$$\dot{m}_{leak1} = \rho \vartheta A_{leak,inlet} C_{leak} \;\; and \;\; \dot{m}_{leak2} = \rho \vartheta A_{leak,outlet} C_{leak} \tag{9}$$

Here, we add these tuning factors to the leakage model. The leakage gap size determines how leakage mass flow rate influences the net mass flow rate of the system. We have observed the amount of leakage is a function of pressure

ratio and volume ratio. Ideal tuning coefficients are generated to perfectly match the experimental data. By using a linear regression on the ideal coefficients, we have established the equation,

$$C_{leak} = 0.1074 + (0.4259 \times Pressure\ Ratio) - (0.033 \times Volume\ Ratio) \quad (10)$$

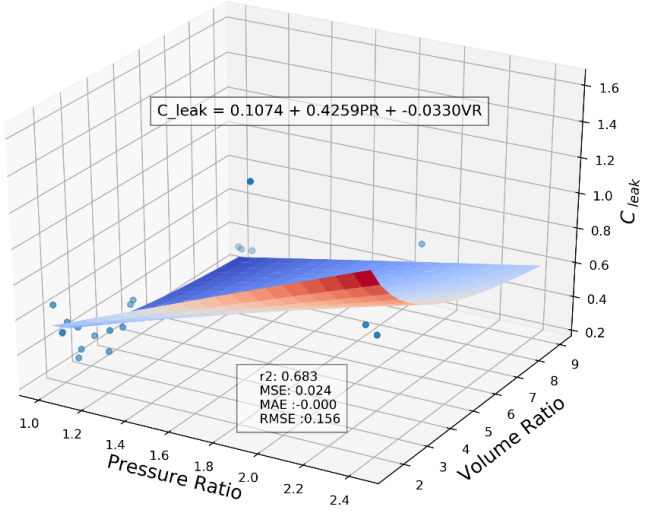

Figure 7: Regression analysis to determine the C_{leak} relation.

By using Equation 10, the mass flow rates from the mechanistic chamber model for all the test points are adjusted, appropriately. The resulting mass flow rate is compared against the experimental measurements with Mean Absolute Percentage Error (MAPE) within 10%. This is shown in Figure 8 which displays a parity plot of the experimental mass flow rate compared against the model predicted values with experimental uncertainty.

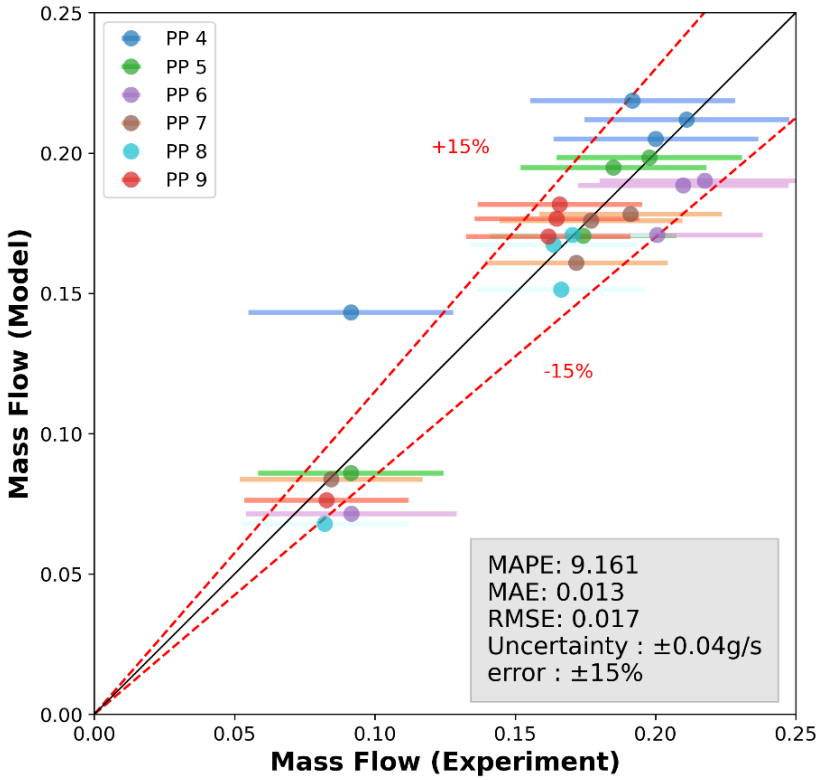

Figure 8: Comparison of experimental and computational mass flow rate.

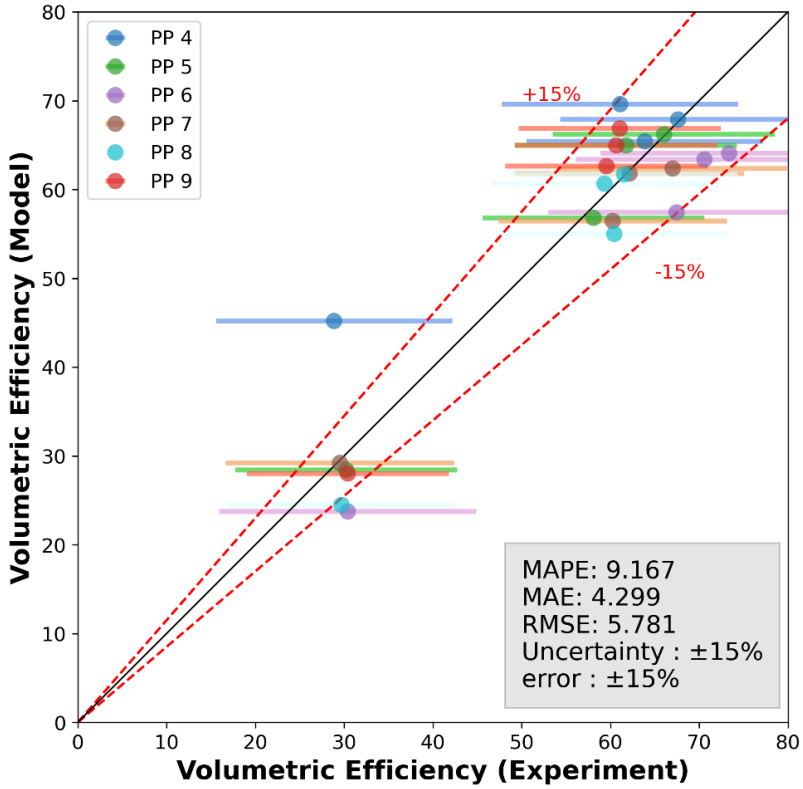

Figure 9: Comparison of experimental and computational volumetric efficiency.

The volumetric efficiency of the compressor depends on the mass flow rate and the compressor speed. The uncertainty for the volumetric efficiency varies from 13.8-15% and the MAPE for the results is around 9%. Figure 9 shows a comparison of the experimental volumetric efficiency to the model predicted values.

5. CONCLUSION

Significant energy can be saved in vapor compression cycles and industrial air compression with improvements in compressor technologies. The peristaltic compressor presents an adaptable technology that potentially increases the efficiency of the system. This study presents the mechanistic chamber model of a peristaltic compressor including the relevant sub-models and geometry to match a reconfigurable prototype compressor, thermodynamic properties, and mass flow rate. Experimental results of the prototype are presented. The results highlighted the influence of adjusting the volume ratio by adjusting the pivotal piston. The analysis of the results shows the mechanistic chamber model has the ability to predict the mass flow rate of the compressor within 10% for a variety of volume and pressure ratios on air. These validated results will allow predicting the most appropriate mechanical activation technology and various design parameters such as different aspect ratios of the diaphragm, different operating speeds, and conditions for the reconfigurable prototype peristaltic compressor.

NOMENCLATURE

A_C	Area of the compression chamber	r	Radius of the piston/compression chamber
A_d	Area of the deflected segment	S	Axial load
A_l	Leakage area	R_g	Gas constant
A_s	Suction and discharge path area	T	Temperature of the fluid
D	Flexural rigidity	V	Volume of the compression chamber
E	Young modulus	Y	Width of the piston
Ma	Mach number	Z	Displacement of the piston
$\dot{m}_{in}$	Mass flow in	ρ	Density of the fluid
$\dot{m}_{out}$	Mass flow out	ϑ	Fluid velocity
$\dot{m}_{leak1}$	Mass flow leakage at inlet	γ	Specific heat
$\dot{m}_{leak1}$	Mass flow leakage at outlet	μ	Poison ratio
P	Pressure of the fluid	ΔF	Load on the diaphragm

REFERENCES

Ahamed, J. U., Saidur, R., & Masjuki, H. H. (2011). A review on exergy analysis of vapor compression refrigeration system. *Renewable and Sustainable Energy Reviews*, *15*(3), 1593–1600. https://doi.org/10.1016/j.rser.2010.11.039

Bell, Ian H., Wronski, J., Quoilin, S., & Lemort, V. (2014). Pure and Pseudo-pure Fluid Thermophysical Property Evaluation and the Open-Source Thermophysical Property Library CoolProp. *Industrial & Engineering Chemistry Research*, *53*(6), 2498–2508. http://pubs.acs.org/doi/abs/10.1021/ie4033999

Bell, Ian Hadley, Ziviani, D., Lemort, V., Bradshaw, C. R., Mathison, M., Horton, W. T., Braun, J. E., & Groll, E. A. (2020). A general quasi-steady modeling approach for positive displacement compressors and expanders. *International Journal of Refrigeration*, *110*, 310–322.

Bradshaw, C. R. (2017). *Development of a Novel Peristalitc Compressor for Air Conditioning Applications. ASHRAE 019-1819. Funding Source: ASHRAE Innovative Research Grant. Project Dates: S. 2019-present*.

Hartley, F. T. (1999). Micropump technology and applications. *Electronics and Structures for MEMS*, *3891*(September 1999), 403–409. https://doi.org/10.1117/12.364470

Huang, C. W., Huang, S. Bin, & Lee, G. Bin. (2006). Pneumatic micropumps with serially connected actuation chambers. *Journal of Micromechanics and Microengineering*, *16*(11), 2265–2272. https://doi.org/10.1088/0960-1317/16/11/003

Islam, M, Tubbs, C., Bengs, C., & Bradshaw, C. R. (2021). Development of a Reconfigurable Prototype Peristaltic Compressor. *IOP Conference Series: Materials Science and Engineering*, *1180*(1), 012046. https://doi.org/10.1088/1757-899x/1180/1/012046

Islam, Mazharul, & Bradshaw, C. R. (2021). *Development of a Mechanistic Chamber Model of a Novel Peristaltic Compressor for Air-conditioning and Refrigeration Applications*.

Lawless, W. N., Arenz, R. W., Cross, L. E., Lawless, W. N., & Arenz, R. W. (1987). *Miniature , solid-state gas compressor Miniature , solid-state gas compressor*. *1487*.

Pearson, A. (2015). What does the future hold for compressor manufacturers? *Proceedings of the Institution of Mechanical Engineers, Part E: Journal of Process Mechanical Engineering*, *229*(2), 88–95. https://doi.org/10.1177/0954408914564814

Sulfridge, M. A., & Miller, N. R. (2001). *The Mesoscopic Peristaltic Compressor*. *61801*(January).

Tanveer, M. M., & Bradshaw, C. R. (2020). Quantitative and qualitative evaluation of various positive-displacement compressor modeling platforms. *International Journal of Refrigeration*, *119*, 48–63. https://doi.org/10.1016/j.ijrefrig.2020.07.009

Timoshenko, S. , Krieger, S. (1941). Theory of Plates and Shells. In *Nature* (Vol. 148, Issue 3760). https://doi.org/10.1038/148606a0

U.S. Department of Energy. (2004). *Energy Tips-Compressed Air Suggested Actions:Determine the Cost of Compressed Air for Your Plant*. *August*. www.eere.energy.gov/industry/bestpractices.

U.S. EIA. (2019). *What is the United States' share of world energy consumption?* Frequently Asked Questions (FAQS). https://www.eia.gov/tools/faqs/faq.php?id=87&t=1#:~:text=What is the United States,604 quadrillion Btu in 2019.

ACKNOWLEDGMENTS

The authors gratefully acknowledge support for this work from the ASHRAE Innovative Research Grant (019-1819), Rexel Inc. of Oklahoma City and the Mechanical and Aerospace Engineering department of Oklahoma State University.